A LabVIEW environment to compensate temperature-driven fluctuations in the signal from continuously running spring gravimeters

[+]Bruno Andò and [++]Daniele Carbone

+ Dipartimento di Ingegneria Elettrica Elettronica e dei Sistemi, Università degli Studi di Catania, V.le A. Doria, 6, 95125 - CATANIA - ITALY, e-mail :bruno.ando@diees.unict.it

++ Istituto Nazionale di Geofisica e Vulcanologia, Sez. di CATANIA, P.zza Roma, 2, 95100 - Catania - ITALY, e-mail: carbone@ct.ingv.it

Corresponding author: Bruno Andò

Abstract

Environmental parameters can seriously affect the performances of continuously running spring gravimeters. Temperature is a primary interfering quantity and its effect must be reduced through algorithms implementing a suitable compensation scheme. Algorithms to reduce the signals coming from continuously running gravimeters for the effect of meteorological perturbations have been developed and implemented in tools running in offline mode.

The need for "on the fly" processing emerges when the recorded signals are used for volcano monitoring purposes, since any information on the volcanic phenomena under development must be assessed immediately. In this paper the implementation, in a dedicated LabVIEW application, of an algorithm performing temperature reduction on gravity signals is discussed and features of the software's user interface are presented.

Keywords: Gravimeter, temperature reduction, compensation algorithm, on-the-fly processing.

Abbreviations:

CTG: Compensation Tool for Gravimeters

PTT: Processing and Test Tool

MOST: Model Order Selection Tool.

Introduction

Mt Etna volcano (Sicily, south of Italy), is covered with several networks of sensors aimed at detecting changes in those physical and chemical parameters which are relevant for monitoring and forecasting purposes (Bonaccorso et al., 2004). To assess meaningful anomalies, some instruments need to be placed as close as possible to the active craters. Unfortunately, the conditions at such sites (high altitude, inaccessibility for several months at a time, lack of mains electricity for power, high peak-to-peak diurnal and seasonal temperature changes, high seismicity) are far from the laboratory standard, and thus is difficult to obtain the required precision of the data (Torge, 1989).

Microgravity studies are performed at active volcanoes to detect underground mass redistributions which may supply important information on the dynamics behind the volcanic activity. These studies are mainly accomplished through spring gravimeters since, with respect to superconducting meters or devices which operates by using the free-fall method (Yoshida et al., 1997; Imanishi, 2001; Imanishi et al., 2004), they are cheaper, smaller (thus easier to transport and install) and take much less power to work. Past studies demonstrated that some external parameters can dramatically affect the behaviour of spring gravimeters (Doebelin, 1985; El Wahabi et al., 1997). It should be emphasized that, since very low variations in the amplitude of the gravity field are to be observed (of the order of a few to a few tens of μGal; 1 μGal=10^{-8} ms^{-2}), sensors with high sensitivity and high resolution must be adopted, which are more prone to the effect of ambient parameter fluctuations (Andò et al., 2004).

In particular, Carbone et al. (2003) proved that, over a yearly period, temperature changes can cause an instrumental effect up to 10^3 μGal. An admittance up to 200 μGal/°C, over the seasonal period, was evidenced by El Wahabi et al. (1997). It is now well established that apparent gravity changes depend on the temporal development and magnitude of the meteorological change that caused them, as well as on the insulation and compensation of the spring gravimeter utilized. Thus, the correction formulas are instrument-specific and often frequency-dependent (Carbone et al., 2003). Accordingly, dedicated approaches must be followed in order to reduce the signal from a continuously running gravity meter for the effect of meteorological parameters.

Andò and Carbone (2001) investigated the possibilities of a Neuro-Fuzzy algorithm as a tool for reducing the gravity signal from a remote Etna station for the effect of meteorological perturbations (namely atmospheric temperature and pressure). Successively, the capabilities of the same compensation algorithm were tested using the signals from three different instruments, recording simultaneously for 50 days at a site far away from active zones, where gravity changes of geodynamic origin were not expected (Andò and Carbone, 2004). The reduced output from the three instruments (after the implementation of the compensation strategy) was within 15 μGal at the 99% confidence interval, and was uncorrelated with temperature. The global validity of the compensation strategy was discussed by Andò and Carbone (2006), who used records from the same instrument operating in different monitoring sites. It was demonstrated the local validity of the compensation model, in spite of the same instrumental setup being utilized implying that different working conditions at the monitoring site mean a different transfer function between perturbing and perturbed signals.

The above cited experiences prove the possibilities of the adopted methodology as a tool for compensating the signal from continuously running gravimeters for the effect of meteorological perturbations.

When the recorded signals are used for volcano monitoring purposes, the need arises for a tool able to implement "on-the-fly" the temperature compensation algorithms.

In this work a tool, hereinafter the *Compensation Tool for Gravimeters (CTG)*, aimed at reducing the output signal from a gravimeter for the effect of temperature, is presented. This tool can be easily integrated in a LabVIEW application already developed and aimed at handling the data coming from remote continuous gravity stations (Carbone, 2002). The *CTG* is intended as a tool for volcano monitoring designed to handle short-lasting sequences (of the order of a few days), i.e. the very last data coming from the remote stations. The compensation strategy adopts a dynamic model implemented into the LabVIEW *CTG* tool through a Matlab® routine exploiting the Matlab® identification toolbox.

The *CTG* can process data from any monitoring site, once a suitable tuning procedure is accomplished, as already evidenced by Andò and Carbone (2001; 2004). In order to suitably tune the compensation strategy, two additional tools are implemented, the *Processing and Test Tool (PTT)* and the *Model Order Selection Tool (MOST).*

The aim of the *PTT* is twofold: (i) it implements algorithms to pre-process the data sequences that will serve as an input to the *MOST*; (ii) furthermore, once the order of the analytical model implementing the temperature reduction from the gravimetric signal is selected, it allows to evaluate the performance of the compensation strategy. The most suitable model order can be selected through the *MOST*. Considering that the model order could be strictly dependent on the monitoring site, the *MOST* should be used every time a new station is installed.

Once the tuning phase has been accomplished, the gravity signal coming from a remote site can be reduced for the effect of temperature fluctuations using the *CTG,* as sketched in Figure 1.

2. The strategy for temperature compensation

The strategy, implemented in the CTG tool and aimed at reducing the gravity signal for the effect of temperature (Andò and Carbone, 2001; 2004), is presented in Figure 1.

As a first step, a model between the gravimeter output, *G,* and temperature *T*, is estimated.

When a good identification of this model is obtained, the residual, *R,* between the effect of temperature variations, simulated by the model, $\hat{G}$, and the meter output, *G*, is calculated:

$$R = G - \hat{G} \tag{1}$$

Performing the interference compensation sketched in Figure 1 allows splitting the meter output into two pieces of information. The first, $\hat{G}$, represents the component of the signal due to the temperature variations while the second, *R*, is correlated to all the other possible causes and represents the reduced signal.

It must be highlighted that dynamics associated to real gravity changes cannot be estimated by the model due to its intrinsic structure (which does not use the output signal from the gravimeter as an input), thus guaranteeing that the information related to subsurface mass redistributions is contained in *R*, as well as the effect of other unconsidered exogenous parameters.

The following prediction-error model structure is used to correlate *G* and *T* signals (Ljung, 1987):

$$G(t) = \frac{B(q)}{F(q)} T(t - nk) + e(t) \tag{2}$$

where

e(t) is the error signal;

q is the delay operator;

$B(q) = b_1 + b_2 q^{-1} + ... + b_{nb} q^{-nb+1}$;

$F(q) = 1 + f_1 q^{-1} + ... + f_{nf} q^{-nf}$;

and

nb is the zeros number+1;

nf is the poles number+1;

nk is the delay.

The decision to adopt this model form, rather than the Polynomial Form or the Neuro-Fuzzy approach (Andò and Carbone, 2001; 2004), is due to the need for a computational approach which combines efficiency with short computation time. Models with the form (2) are evaluated by the Matlab® identification toolbox.

INSERT FIGURE 1 APPROXIMATELY HERE.

3. Station setup and data pre-processing

The data presented and analyzed in the following were acquired between April and September 2005 at one of the continuous gravity stations of the Etna array (Belvedere, BVD, 2850 m a.s.l., about 1 km from the summit craters). The station is installed inside a semi-underground concrete box (Fig. 2) and is equipped with LaCoste & Romberg D-185 spring gravimeter. A polystyrene box protects the sensor from ambient temperature (Fig. 2).

Besides gravity, other parameters are acquired: ground tilt along two perpendicular directions, atmospheric temperature (inside and outside the box hosting the meter), pressure, humidity and voltage level from the power system feeding the station. Data are collected at 1 datum/min sampling rate (each datum is the average calculated over 60 measurements) through a CR10X Compbell Scientific data-logger and transmitted through a GSM connection to the INGV in Catania. Signals of gravity (reduced for the Earth tide effect) and temperature, acquired at BVD during the April - September 2005 period, are presented in Figure 3.

The effect of Earth tide (amplitude up to 200 μGal peak-to-peak depending on latitude, elevation and stage in the tidal cycle) is removed from the gravity signal through a standard tidal prediction computation, which allows accuracies within ±1% (Wenzel, 1996). This implies tidal residuals affecting the gravity signal up to 1-2 μGal peak-to-peak over the most relevant tidal waves (diurnal and semidiurnal).

Before being processed, gravity data are corrected for the instrumental drift (Torge, 1989). Over short-lasting sequences (up to about 1 month) the instrumental drift over time is modelled as the best linear fit (Carbone et al., 2003).

INSERT FIGURE 2 APPROXIMATELY HERE.

INSERT FIGURE 3 APPROXIMATELY HERE.

4. The *Processing and Test Tool (PTT)*

The *PTT* is utilized both before the model order selection, to prepare the data sequences under study, and afterwards to check the performances of the compensation scheme. The *PTT*'s first section allows to inspect and pre-process the data (gravity and temperature) used to model the effect of temperature on the gravimeter output (Fig. 4a). The operator can interactively decide which data slot will be used and which operations will be applied to the original signal. Operations allowed in the first section of *PTT* are: data filtering and reduction for linear or polynomial trends. Hereinafter, the term *Manipulated* will be used to indicate processed data (the

Gravimeter signal is always reduced for the effect of Earth tide and instrumental drift and, if needed, filtered by the PTT tool).

In order to investigate the correlation between gravimeter output and temperature, which can be dramatic for this kind of instrument, especially over the lowest frequencies (Torge, 1989; El Wahabi et al., 1997; Bonvalot et al., 1998; El Wahabi et al., 2000), a Correlation Analysis can also be carried out through the second section of the *PTT* (Fig. 4b).

The last section of the *PTT* allows for testing the performance of the temperature compensation strategy, once the model order has been selected, as outlined in the next paragraph. The user can verify the effect of the compensation strategy by comparing the manipulated gravimeter output and the reduced sequence (Fig. 5).

INSERT FIGURE 4 APPROXIMATELY HERE.

INSERT FIGURE 5 APPROXIMATELY HERE.

5. The *Model Order Selection Tool (MOST)*

In this section the procedure aimed at retrieving the optimal *nb*, *nf*, *nk* parameters (section 2), which define the model order, is described. This operation is mandatory when a new monitoring station is installed and, in that case, a suitable data set must be collected to perform rigorous model order identification.

In particular, a screening of parameters *nb*, *nf*, *nk* (all the possible combinations of such parameters are considered within a pre-defined range of variation) is performed and each resulting model is tested against weekly sub-sequences (consisting of *N* samples), obtained from the original data set.

In order to estimate the efficiency of each model the following Mean Square Error index has been used, weighting the residuals between the gravimeter output, *G,* and the model estimation, $\hat{G}_{nb,nf,nk}$ for a particular set of *nb*, *nf*, *nk* parameters:

$$J_{nb,nf,nk} = \sqrt{\frac{\sum_{i=1}^{N}(G - \hat{G}_{nb,nf,nk})^2}{N}} \tag{3}$$

where N is the number of for the data samples.

Figure 6 shows the behaviour of this index as a function of the weekly data sequences for different values of the model parameters. It is evident that all models fail for specific weekly sequences (indicated with arrows) implying the possible occurrence of specific problems affecting those data sub-sets (higher than normal teleseismic activity, failure of the power supply system of the gravity station, etc.). Actually, a deeper analysis of the suspected data sequences reveals serious data corruption in the original data set. If the corrupted data are removed, the minimization index values are drastically reduced.

Model order selection is performed by analyzing the average behaviour of the Mean Square Value of the residuals between original and estimated data. The average operator is applied to the set of weekly sequences:

$$J_{Av} = \frac{1}{M}\sum_{q=1}^{M}\sqrt{\frac{\sum_{i=1}^{N}(G - \hat{G}_{nb,nf,nk})^2}{N}} \tag{4}$$

where M is the number of weakly sequences considered, q is the number of weekly sequences and i counts for the data samples.

INSERT FIGURE 6 APPROXIMATELY HERE.

The trend of index J_{Av} is shown in Figure 7, as a function of the model order (each sample is the value of J_{Av} for a given combination of *nb*, *nf*, *nk* parameters). In the case under attention, a good trade off between minimum model order and suitable performances of the compensation strategy is obtained for values of the parameters *nb*, *nf*, *nk* of 5, 9 and 5, respectively (arrows in Figure 7). Figure 8 is a representation of the J_{Av} operator for *nb*=5, which highlights the occurrence of such optimal set of values.

The model order selection procedure is implemented through a Matlab routine which provides the possibility to select a reliable data sub-set. Moreover, the selected optimal model order is provided to the user in a textual form due to the difficulty to perceive such information from the graphical output (see the x-axis of Figure 7). Although this procedure is mandatory when a new monitoring station is installed, it is also advisable to run the model order estimation periodically, to adapt the model form to the last data sequence, hence improving the performances of the compensation strategy. Since this operation can be performed in offline–mode through the *PTT* tool, the efficiency of the monitoring procedure is not compromised.

As stated in section 4, the effectiveness of the selected model structure can be evaluated through the last section of the *PTT* tool (whose interface is shown in Figure 5) which enables the comparison between the gravity signal corrected for Earth Tide and instrumental drift, *G*, and the signal *R*.

Examples of gravimeter sequences reduced for the effect of temperature are given in Figure 9, reporting the comparison between the manipulated gravimeter signal (corrected for earth tide and instrumental drift) and the reduced signal. The comparison between the mean square values for the signals *G* and *R* is presented in Table 1. The instantaneous correlation index between *G* and *T* signals, $\chi(G, T)$, and between *R* and *T* signals, $\chi(R, T)$, are given in Table 2. These results demonstrate the efficiency of the compensation strategy which produces a dramatic reduction of both the absolute signal amplitude and the correlation with temperature fluctuations.

INSERT FIGURE 7 APPROXIMATELY HERE.

INSERT FIGURE 8 APPROXIMATELY HERE.

INSERT FIGURE 9 APPROXIMATELY HERE.

6. The Compensation Tool for Gravimeters

As introduced above, volcano monitoring purposes imply the need for a "on-the-fly" processing able to automatically handle gravity data coming from the monitoring sites and reduce the instrumental effect of temperature fluctuations. To fulfil this need, the *CTG* was realized in the LabVIEW environment (Fig. 10). The

new developed tool uses the data output from a previously developed software (GraVisual; Carbone, 2002) which reduced the gravity signal for the effect of Earth tide and instrumental drift. A selection of the data sequence to be processed by the *CTG* can be performed, the last week being the default choice. The *CTG* performs data filtering on user demand and produces the reduced sequence through implementation of the model form (2). Two filtering operations can be performed on the signal *G* for the model identification task and for the estimation of the residual, respectively. The effect of adopting a filter (which removes changes faster than 2 hours) for the residual estimation task is also presented in Figure 10.

Furthermore, it is important to stress that the convergence time of the developed algorithm (time required for residual calculation (see Figure 1)) is much shorter than the sampling rate at the remote acquisition site (1 datum/min). Operations related to model order identification (data pre-processing and screening of different order models) are off-line procedures which do not affect the "on-the-fly" execution of the temperature compensation procedure.

Finally, on the right-hand side of the user interface (see Figure 10) results of the instantaneous correlation analysis between *G* and *T* and between *R* and *T* is furnished along with the Mean Square Index related to the residual obtained.

Results obtained in terms of both performances of the implemented strategy in reducing the gravimetric signal for the effect of temperature fluctuations (Andò and Carbone, 2001; 2004; 2006) and effectiveness (reliability and flexibility) of the developed LabVIEW environment (CTG, PTT and MOST) encourage the use of this methodology to improve the quality of the information acquired through continuous gravity measurements in active volcanic areas.

INSERT FIGURE 10 APPROXIMATELY HERE.

7. Concluding remarks

It is now well established that fluctuation in ambient temperature can affect the output from spring gravimeters (El Wahabi et al., 2000; Carbone et al., 2003). The instrumental effect driven by temperature is meter/setup specific and frequency-dependent and thus must be removed through non-linear techniques and in a case-by-

case fashion (Andò and Carbone, 2001; 2004; 2006). These issues pose strict constraints on the use of spring gravimeters for volcano monitoring. In fact, to assess meaningful changes, the instruments must be installed close to the active structures, thus often in the summit zone of a high volcano, where fluctuation in ambient temperature can be severe and where the lack of mains electricity prevents active systems, able to stabilize the temperature within an acceptable range, from being utilized. On the other hand, effective volcano monitoring can be performed only if the data from the continuously recording remote stations are immediately available for analysis. The intersection of the above constraints yields the need for a tool able to compensate on-the-fly the last part of the sequences coming from the remote sites for the effect of ambient temperature.

The kernels of a such new tool, which uses a model form developed in previous studies (Andò and Carbone, 2001; 2004), are described in the present work. We are confident that the use of the algorithms and tools presented here will enhance the potential of continuous gravity measurement through spring gravimeters for a valuable monitoring of active volcanoes.

References

Andò, B., Carbone, D., 2001. A Methodology for Reducing a Continuously Recording Gravity Meter for the Effect of Meteorological Parameters. IEEE Trans. On Instrumentation and Measurements, 50 (5), 1248-1254.

Andò, B., Carbone, D., 2004. A test on a Neuro-Fuzzy algorithm used to reduce continuous gravity records for the effect of meteorological parameters. Physics of the Earth and Planetary Interiors, 142, 37-47.

Andò, B., Carbone, D., 2006. A new computational approach to reduce the signal from continuously recording gravimeters for the effect of atmospheric temperature. Physics of the Earth and Planetary Interiors, 159 (3-4), 247-256.

Andò, B., Coltelli, M., Sambataro, M., 2004. A Measurement Tool for Investigating Cooling Lava Properties, IEEE Trans. on Instrumentation and Measurements, 53 (2), 507-513.

Bonaccorso, A., Calvari, S., Coltelli, M., Del Negro, C., Falsaperla, S., (eds.), 2004. Mt. Etna: Volcano Laboratory, Geophysical Monograph Series 143, 384 pp.

Bonvalot, S., Diament, M., Germinal, G., 1998. Continuous gravity recording with Scintrex CG-3M meters: a promising tool for monitoring active zones. Geophysical Journal International, 135, 470-494.

Carbone, D., 2002. Gravity monitoring of Mount Etna (Italy) through discrete and continuous measurements. Ph.D. Thesis, The Open University, Milton Keynes, U.K.

Carbone, D., Budetta, G., Greco, F., Rymer, H., 2003. Combined discrete and continuous gravity observations at Mount Etna, Journal of volcanology and geothermal research, 123, 123-135.

Doebelin, E. O., 2003. Measurement Systems, 5th ed, McGraw-Hill pp. 768.

El Wahabi, A., Ducarme B., Van Ruymbeke M., d'Oreyè N., Somerhausen A., 1997. Continuous gravity observations at Mount Etna (Sicily) and Correlations between temperature and gravimetric records, Cahiers du Centre Européen de Géodynamique et de Séismologie, 14, 105-119.

El Wahabi, A., Dittfeld, H.J., Simon, Z., 2000. Meteorological in£uence on tidal gravimeter drift. Bull. Inf. Marées Terr., 133, 10403-10414.

Imanishi, Y., 2001, Development of a high-rate and high-resolution data acquisition system based on a real-time operating system, J. Geod. Soc. Japan, 47, 52-57.

Imanishi, Y., Tadahiro, S., Toshihiro, H., Wenke, S., Okubo, S., 2004. A Network of Superconducting Gravimeters Detects Submicrogal Coseismic Gravity Changes. Science, 306, 476-478

Ljung, L, 1999. System Identification - Theory For the User, 2nd ed, PTR Prentice Hall, Upper Saddle River, N.J.

Torge, W., 1989. Gravimetry. Walter de Gruyter., Berlin-New York.

Wenzel, H.G., 1996. The nanogal software: Earth tide data processing package ETERNA 3.30. Bull. Inf. Marées Terr., 124, 9425-9439.

Yoshida, S., Gaku, S., Okubo, S., Kobayashi, S., 1997. Absolute gravity change associated with the March 1997 earthquake swarm in the Izu Peninsula, Japan. Earth Planets Space, 51, 3–12.

Figure Captions

Figure 1. Scheme of the compensation environment.

Figure 2. The set-up of a gravity station on Etna.

Figure 3 – Signals acquired at BVD gravity station between April 2005 and September 2005. (a) Gravimeter output, (b) Ambient temperature.

Figure 4. The first two Sections of the Processing and Test Tool. (a) Data pre-processing section; (b) correlation analysis section.

Figure 5. The third Section of the Processing and Test Tool performing temperature compensation.

Figure 6. The $J_{nb,nf,nk}$ index as a function of weekly data sequences for different values of the model parameters.

Figure 7. The J_{Av} index for different combinations of the model order parameters nb, nf, nk.

Figure 8. The J_{Av} index for the case nb=5. As indicated by the arrow a suitable model order is given by nb=5, nf=9 and nk=5.

Figure 9. The comparison between Manipulated Gravimeter Output and the Reduced Signal for different weekly sequences.

Figure 10. The effect of filtering the G signal for the Residual estimation task.

Table 1. Mean square index of signals G and R for the weekly sequences shown in Figure 9.

Table 2. Instantaneous correlation index between G and T signals and between R and T signals, for the weekly sequences shown in Figure 9.

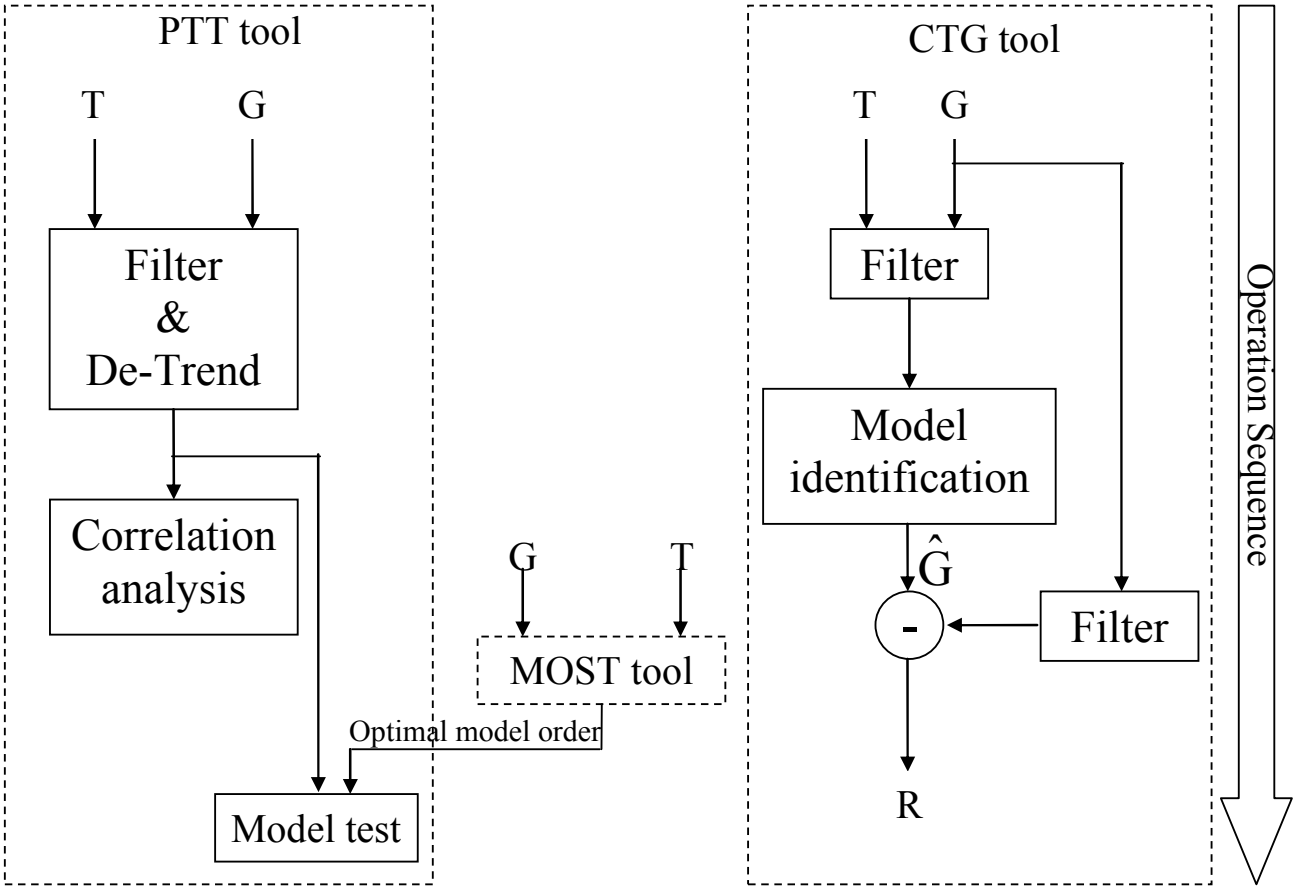

Figure 1. Scheme of the compensation paradigm.

Figure 2. The set-up of a gravity station on Etna.

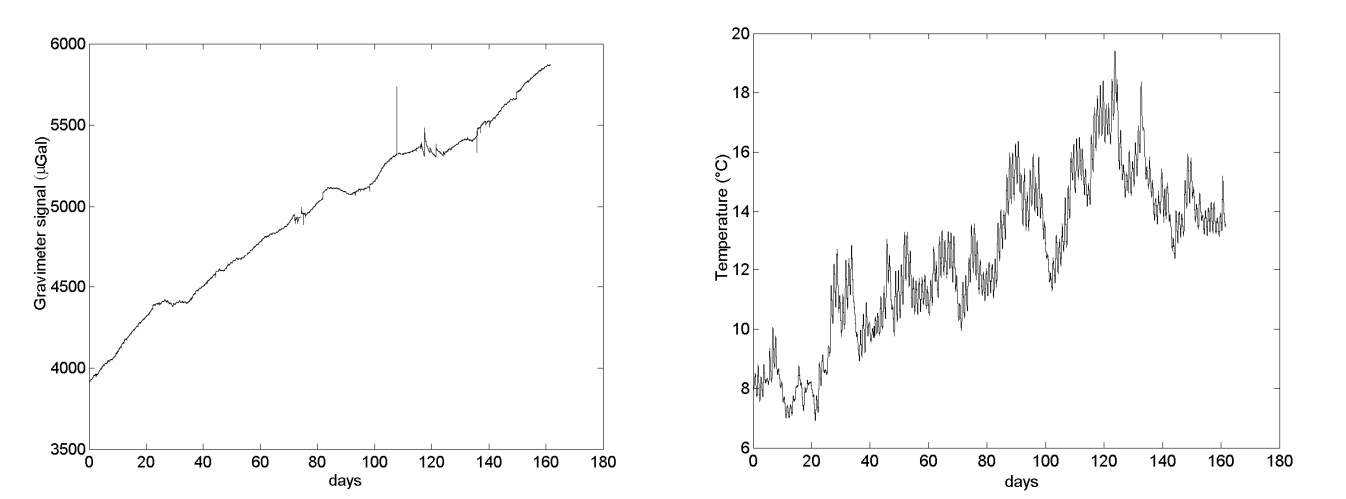

Figure 3 – Signals acquired at BVD gravity station between April 2005 and September 2005. (a) Gravimeter output, (b) Ambient temperature.

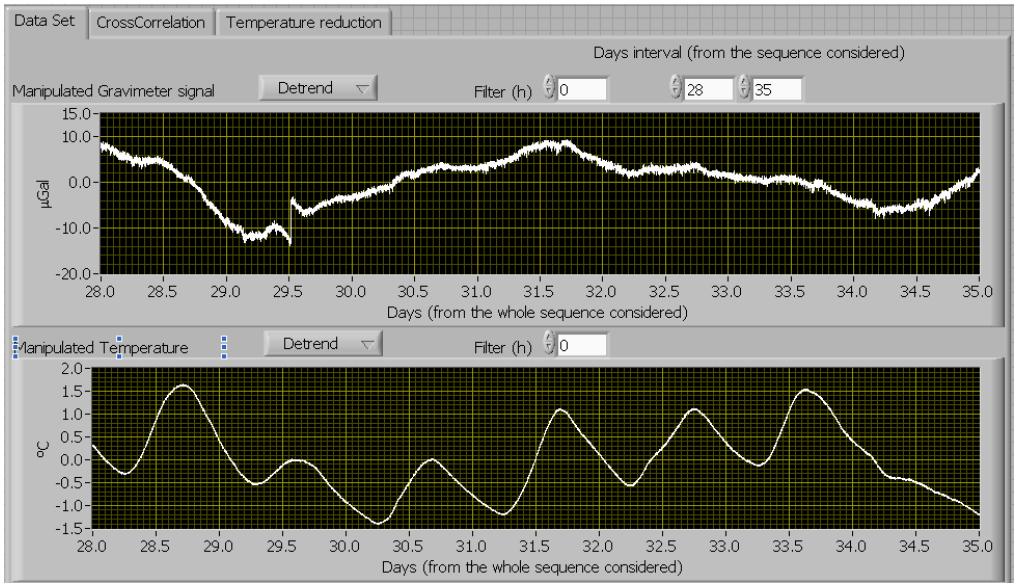

(a)

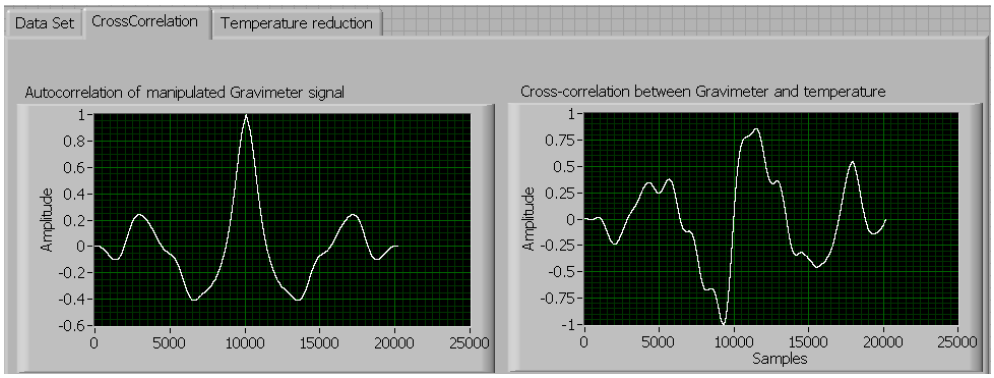

(b)

Figure 4. The first two Sections of the Processing and Test Tool. (a) Data pre-processing section; (b) correlation analysis section.

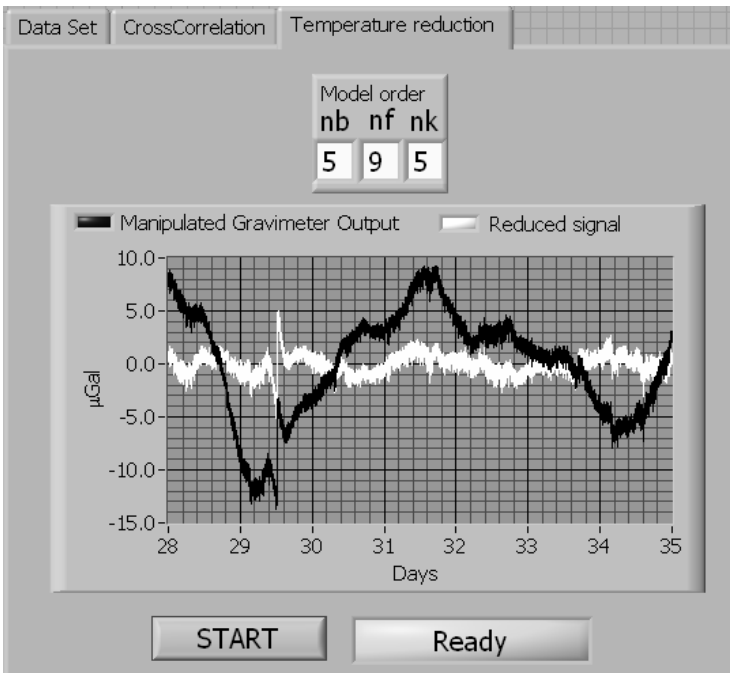

Figure 5. The third Section of the Processing and Test Tool performing temperature compensation.

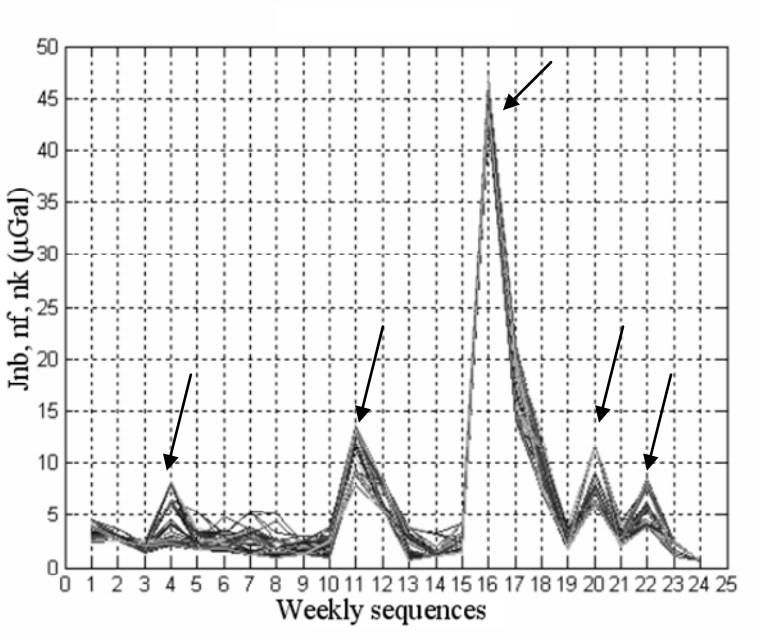

Figure 6. The $J_{nb,nf,nk}$ index as a function of weekly data sequences for different values of the model parameters.

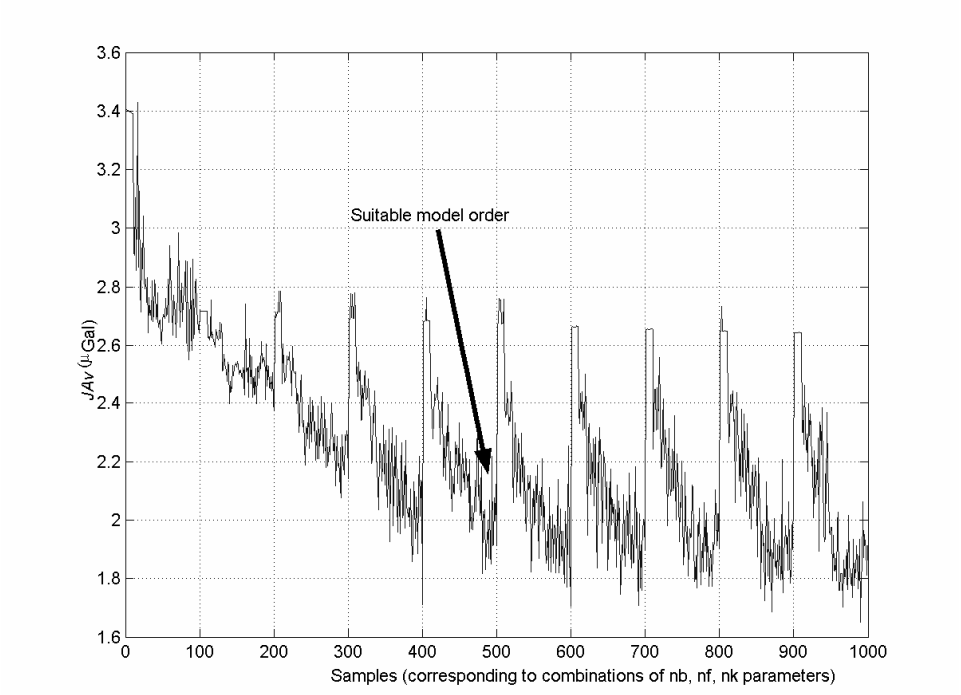

Figure 7. The J_{Av} index for different combinations of the model order parameters nb, nf, nk.

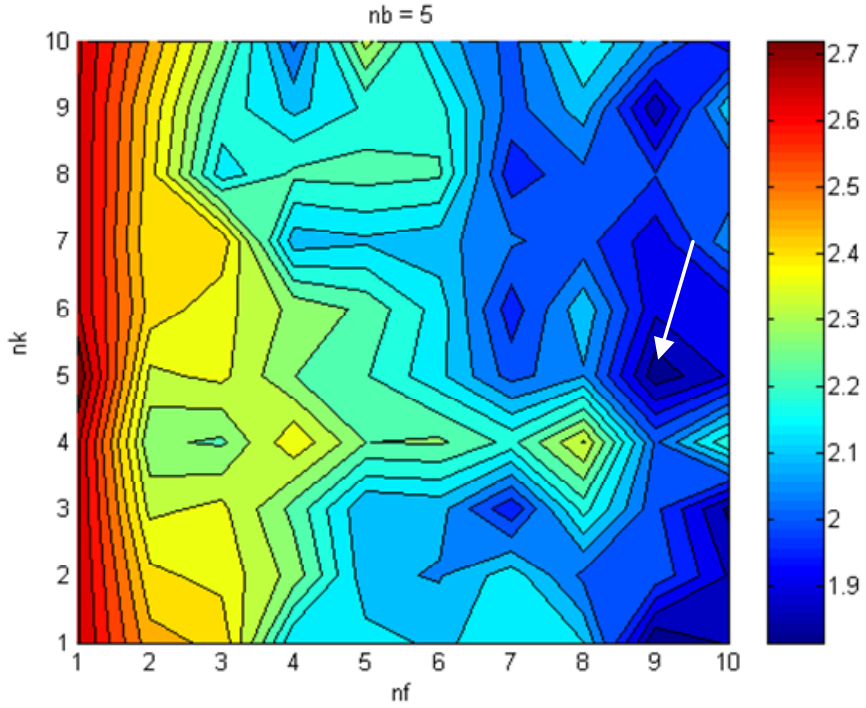

Figure 8. The J_{Av} index for the case nb=5. As indicated by the arrow a suitable model order is given by nb=5, nf=9 and nk=5.

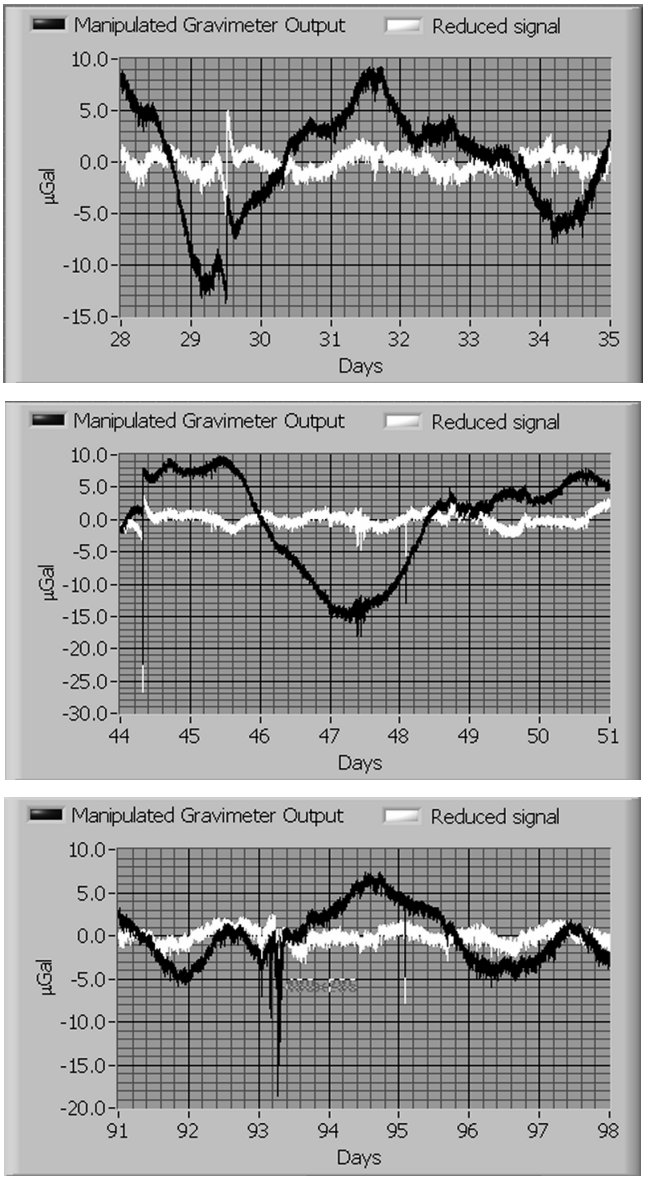

Figure 9. The comparison between pre-filtered gravimeter output and the reduced signal for different weekly sequences.

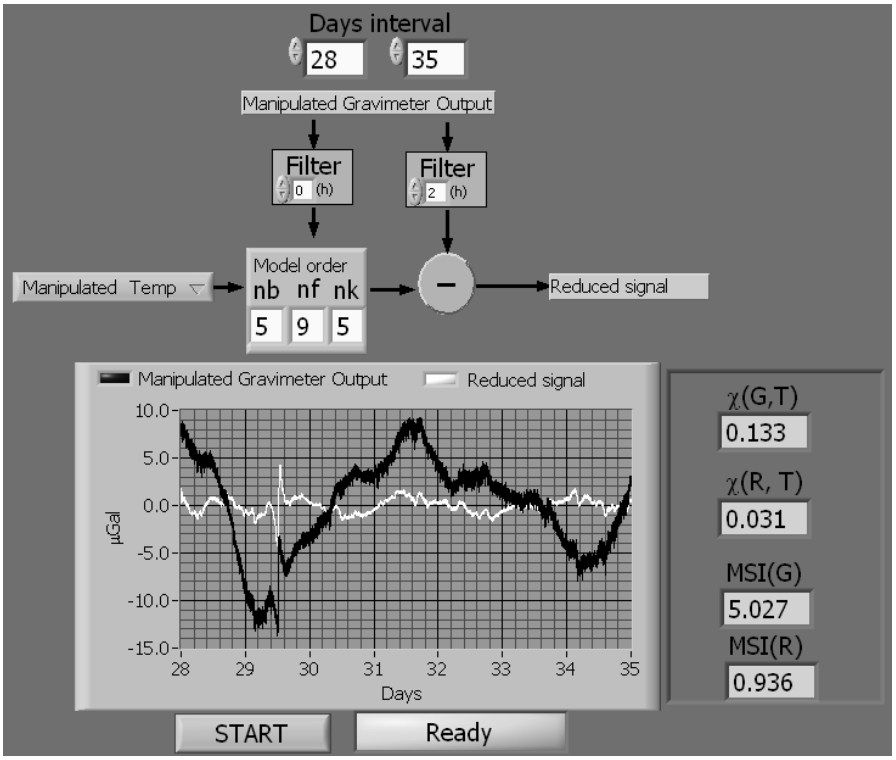

Figure 10. The effect of filtering the G signal for the Residual estimation task.

Sequence (days)	*MSI(G)*	*MSI(R)*
28-35	5.06	1.70
44-51	7.33	1.06
91-98	3.25	1.13

Table 1. Mean square index of signals G and R for the weekly sequences shown in Figure 9.

Sequence (days)	$\chi(G, T)$	$\chi(R, T)$
28-35	0.299	0.012
44-51	0.087	0.013
91-98	0.294	0.006

Table 2. Instantaneous correlation index between G and T signals and between R and T signals, for the weekly sequences shown in Figure 9.